Influence of coastal vegetation on the 2004 tsunami wave impact in west Aceh

Juan Carlos Laso Bayas[a], Carsten Marohn[a], Gerd Dercon[a,1], Sonya Dewi[b], Hans Peter Piepho[c], Laxman Joshi[b], Meine van Noordwijk[b], and Georg Cadisch[a,2]

[a]Institute of Plant Production and Agroecology in the Tropics and Subtropics, University of Hohenheim, 70593 Stuttgart, Germany; [b]World Agroforestry Centre, Southeast Asia Regional Program, P.O. Box 161, Bogor 16001, Indonesia; and [c]Institute of Crop Science, University of Hohenheim, 70593 Stuttgart, Germany

Edited* by William C. Clark, Harvard University, Cambridge, MA, and approved July 12, 2011 (received for review September 27, 2010)

In a tsunami event human casualties and infrastructure damage are determined predominantly by seaquake intensity and offshore properties. On land, wave energy is attenuated by gravitation (elevation) and friction (land cover). Tree belts have been promoted as "bioshields" against wave impact. However, given the lack of quantitative evidence of their performance in such extreme events, tree belts have been criticized for creating a false sense of security. This study used 180 transects perpendicular to over 100 km on the west coast of Aceh, Indonesia to analyze the influence of coastal vegetation, particularly cultivated trees, on the impact of the 2004 tsunami. Satellite imagery; land cover maps; land use characteristics; stem diameter, height, and planting density; and a literature review were used to develop a land cover roughness coefficient accounting for the resistance offered by different land uses to the wave advance. Applying a spatial generalized linear mixed model, we found that while distance to coast was the dominant determinant of impact (casualties and infrastructure damage), the existing coastal vegetation in front of settlements also significantly reduced casualties by an average of 5%. In contrast, dense vegetation behind villages endangered human lives and increased structural damage. Debris carried by the backwash may have contributed to these dissimilar effects of land cover. For sustainable and effective coastal risk management, location of settlements is essential, while the protective potential of coastal vegetation, as determined by its spatial arrangement, should be regarded as an important livelihood provider rather than just as a bioshield.

glimmix | tsunami mitigation | vegetation effects | food security

On December 26, 2004, a rupture in the fault line between the Indo-Australian and southeastern Eurasian tectonic plates 150 km off the coast of west Aceh, Indonesia, triggered one of the largest seismic events in the last four decades (1). The seaquake generated a tsunami with disastrous consequences in the region.

Soon after the 2004 event, the possible effects of coastal vegetation regarding the impact caused by tsunamis (mitigating or aggravating) were researched into, especially under scenarios with initial water heights below 10 m (2–5). In Sri Lanka and India, coastal communities located behind tree cover were reported to be less affected than those directly exposed to the sea (2, 3, 6). Parameters such as stem diameter and height as well as a "bioshield" width were identified as key vegetation characteristics with a bearing on impact mitigation (6). However, several studies advocating bioshields have been criticized for lacking empirical evidence to support the protective function of vegetation, some even suggesting that bioshields may give a false sense of security to coastal populations (7–10). The role of vegetation in tsunami impact mitigation still remains a controversial issue (11–13). In the coastal regions of western Aceh in 2004, the potential for mitigating tsunami impacts appeared limited as a result of the massive energy released by waves with heights exceeding 20 m (13). Mangroves along this coastline were naturally scarce because this is a high energy coastline in contrast to locations in Thailand and Sri Lanka. Dense natural vegetation had been replaced by cultivated (tree and annual) crops, rubber agroforests being the most forest-like. Nevertheless, soon after the tsunami, afforestation programs were launched to reduce the impact of possible future tsunami flood events (14). Many of these plans overlooked local needs and acceptance of such solutions, therefore compromising their future maintenance.

This study assessed the effectiveness of coastal vegetation in mitigating the wave impact caused by the tsunami event of 2004 in part of the west coast of Aceh. The role of vegetation behind villages, which had been previously reported as relevant by local informants, was particularly considered.

The intensity of damage caused by a tsunami depends not only on the strength of the seaquake and offshore properties but also on landscape characteristics such as coastal geomorphology, topography, and land cover (15, 16). Once a tsunami wave train arrives inland, its energy is dissipated by gravitational forces and friction (17). The remaining wave energy determines the effects experienced inland—i.e., maximum flood distance, human casualties, and structural damage to buildings. Therefore, the utility of initial water height at shoreline (as proxy for wave energy), elevation at point of impact (gravitation) and land cover roughness (including vegetation friction) (2, 18) as predictors of inland damage was assessed using spatially explicit statistical models.

On the west coast of Aceh sample sites were identified using satellite imagery (Fig. 1). Differences in observed initial water height pointed to offshore factors affecting the wave energy arriving at the shore. Consequently, initial water height at the shoreline (IWH) was used to represent initial wave energy. Topography was represented by elevation (E); the area is a relatively homogeneous coastal plain with gentle slopes between 0.2 and 4.5%. Information on IWH, land cover changes and damage indicators was collected on site during interviews with over 200 groups of eyewitnesses, a literature review, and from satellite images (details see *Methods*). Such data was correspondingly assigned to each of the 180 transects perpendicular to the coastline, used as study units. The different land cover types present in the transects were afterwards transformed to a vegetation resistance index—i.e., land cover roughness (LCR).

Multifactorial approaches describing resistance of vegetation to a flow (6, 19, 20) are usually highly data-demanding. Conse-

Author contributions: J.C.L.B., C.M., G.D., M.v.N., and G.C. designed research; J.C.L.B. performed research; J.C.L.B., S.D., H.P.P., and G.C. contributed new reagents/analytic tools; J.C.L.B. analyzed data; and J.C.L.B., C.M., G.D., S.D., H.P.P., L.J., M.v.N., and G.C. wrote the paper.

The authors declare no conflict of interest.

*This Direct Submission article had a prearranged editor.

Freely available online through the PNAS open access option.

[1]Present address: Joint FAO/IAEA Division of Nuclear Techniques in Food and Agriculture, Department of Nuclear Sciences and Applications, International Atomic Energy Agency, Wagramerstrasse 5, 1400 Vienna, Austria.

[2]To whom correspondence should be addressed. E-mail: georg.cadisch@uni-hohenheim.de.

This article contains supporting information online at www.pnas.org/lookup/suppl/doi:10.1073/pnas.1013516108/-/DCSupplemental.

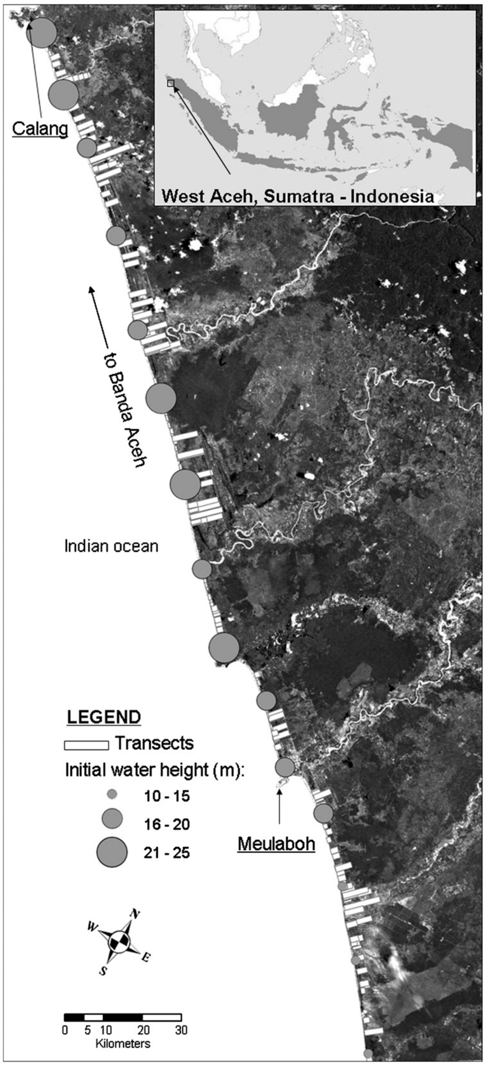

Fig. 1. Study area: transects and initial water height along the coast (Landsat® ETM).

quently, a set of characteristics was identified that were not only comparatively easy to quantify on site but also able to sufficiently represent the resistance of specific land uses. The maximum bending moment, a measure of resistance, is highly correlated with tree height, diameter at breast height, and with the material-specific "modulus of elasticity" (21). Empirically, the main force that different types of trees (vegetation) oppose to water mass flows could therefore be approximated by combining information on stem diameter and stand height. By including planting density, the vegetation resistance coefficient (VR) in $m^3\,ha^{-1}$ at stand level can be defined as:

$$\mathrm{VR} = \mathrm{H} \times \mathrm{SD}^2 \times \mathrm{d}, \qquad [1]$$

where $\mathrm{H} =$ vegetation height (m), $\mathrm{SD} =$ stem diameter at breast height (trees) or at ground level (nontree vegetation) (m) and $\mathrm{d} =$ planting (number of individuals per area).

Height, stem diameter, and planting density were measured in the field on corresponding land uses of comparable age class and characteristics as the ones affected by the tsunami (details see *Methods*).

The sum of vegetation resistance coefficients per land use type multiplied by their respective area in each transect (Fig. 1)—i.e., the cumulative land cover roughness ($\sum$ LCR in m^3)—was then calculated as:

$$\sum \mathrm{LCR} = \mathrm{VR}_1 \times \mathrm{A}_1 + \mathrm{VR}_2 \times \mathrm{A}_2 + \ldots + \mathrm{VR}_n \times \mathrm{A}_n, \qquad [2]$$

where $\mathrm{VR}_{(1\rightarrow n)} =$ specific resistance coefficient for any given land use ($m^3\,ha^{-1}$), and $\mathrm{A}_{(1\rightarrow n)} =$ area (ha) covered by the respective land use in a transect.

$\sum$ LCR includes distance, and because distance from the shoreline has commonly been reported to influence tsunami impacts, $\sum$ LCR was normalized by division over total transect area. The resulting weighted average land cover roughness coefficient (LCR) was used for all models:

$$\mathrm{LCR} = [\mathrm{VR}_1 \times \mathrm{A}_1 + \mathrm{VR}_2 \times \mathrm{A}_2 + \ldots + \mathrm{VR}_n \times \mathrm{A}_n] \times \mathrm{A_T}^{-1} \qquad [3]$$

where $\mathrm{A_T} =$ total transect area (ha).

A description of land cover types identified in the study area as well as their respective coefficients are given in Table 1. Community members reported that the vegetation directly behind a settlement influenced the tsunami impact they experienced. Thus, land cover roughness of the first 500 m behind the settlement was evaluated and added as a further predictor ($\mathrm{LCR_{B5}}$) in the impact models (Eqs. **5** and **6**).

Distribution of structural damage (STD) data was nonhomogenous—i.e., mainly split into two categories: "destroyed" or "not significantly affected" (Fig. S1*C*). Therefore, all values bigger than 0 were transformed to 1, creating a binomial response variable STDB. Additionally, values of the predicted variable casualties (CASU) and maximum flood distance (MD) were transformed from a scale of 0 to 100 to a scale of 0 to 1 (CASU01 and MD01, respectively). Finally, all predictors in each model were standardized to mean 0 and variance 1. Therefore, the three tsunami impact models, each using a total of 180 observations, were:

$$\mathrm{MD01} = f(\mathrm{IWH\text{-}s}, \mathrm{E_T\text{-}s}, \mathrm{LCR_T\text{-}s}), \qquad [4]$$

$$\mathrm{CASU01} = f(\mathrm{IWH\text{-}s}, \mathrm{D\text{-}s}, \mathrm{E_F\text{-}s}, \mathrm{LCR_F\text{-}s}, \mathrm{LCR_{B5}\text{-}s}), \qquad [5]$$

and

$$\mathrm{STDB} = f(\mathrm{IWH\text{-}s}, \mathrm{D\text{-}s}, \mathrm{E_F\text{-}s}, \mathrm{LCR_F\text{-}s}, \mathrm{LCR_{B5}\text{-}s}), \qquad [6]$$

where suffix $\text{-s} =$ standardized, $\mathrm{IWH\text{-}s} =$ initial water height at shoreline (m), $\mathrm{E_T\text{-}s} =$ maximum elevation over the whole flooded transect (m a.s.l.), $\mathrm{LCR_T\text{-}s} =$ weighted average land cover roughness in the transect (up to the maximum flood distance), $\mathrm{D\text{-}s} =$ distance from the settlement to the shoreline (m), $\mathrm{E_F\text{-}s} =$ maximum elevation at the settlement level (m a.s.l.), $\mathrm{LCR_F\text{-}s} =$ weighted average land cover roughness from the settlement to the shoreline and $\mathrm{LCR_{B5}\text{-}s} =$ weighted average land cover roughness from the settlement up to 500 m behind.

Variables description and summary statistics are shown in Table 2, and a schematic representation of model parameters can be seen in Fig. 2.

Data were expected to be spatially correlated because of dense sampling along the coastline. Also, some response variables violated the usual assumptions of normality and homoscedasticity (Fig. S1*B* and *C*). In order to account for these factors, we fitted spatial Generalized Linear Mixed Models (GLMM) by maximum and pseudolikelihood methods (27). The Akaike Information Criterion (AIC) was used as a measure of goodness of fit for the maximum flood distance and casualty models. In the binomial GLMM for structural damage, Pearson's chi-squared statistic divided by the degrees of freedom was used as a measure of model fit. Pearson residuals from spatial GLMMs for structural damage, casualties, and maximum flood distance were checked for remaining spatial dependencies. Moran's test I ($I = 0.02$; Z

Table 1. Land cover types, area covered in study transects, planting densities, and vegetation resistance coefficients (VR), west coast of Aceh (Calang to south of Meulaboh)

Land-cover type	Area covered (%)	Estimated planting density (stems ha^{-1})	VR* (m^3 ha^{-1})
Cleared land: areas with no vegetation	0.63	0	0
River: water areas including ponds and estuaries	3.33	0	0
Agriculture: various crops, mostly vegetable plantations	0.03	31,250	13
Grass: planted or natural grassland, e.g., *Imperata spp.*	8.34	2,000,000	15
Rice field: plantations of *Oriza sativa*, usually paddies	19.04	2,000,000	15
Shrub: Natural vegetation of 1 to 2 m height	0.01	4,445	150
Cocoa: plantations of *Theobroma cacao*	1.99	1,111	156
Coconut: plantations of *Cocos nucifera*	20.46	156	281
Oil palm: plantations of *Elaeis guineensis*	4.45	156	366
Agroforest: combinations of different plant species†	6.34	625	844
Rubber: *Hevea brasiliensis*, mostly extensive jungle rubber	16.72	494	1,343
Forest: local timber and non timber species on protected and nonprotected areas	0.24	494	2,099
Settlements	17.11	N/A	3,538‡

Obtained from Landsat® ETM 2002 land cover classification.

Around 1% of the area was nonidentifiable on satellite imagery (classified either as cloud, shadow, or no data).

*m^3 ha^{-1} refers to volume of plants (stems) resisting the force of water advancing per hectare. See Eq. **1**.

†Canopies at various levels, e.g., mango (*Mangifera indica*), coffee (*Coffea arabica*), sugar (*Saccharum spp.*), and vegetables.

‡For the land-cover "settlements" values of modulus of elasticity (MOE) of wood, concrete, and grasses reported in several studies (21–26) were compared. A VR value was then derived based on the transformed values for concrete Compressive Strength (CE) of the buildings in Aceh. Before the tsunami, buildings in Aceh had a CE of around 10 to 12.5 MPa (33) (MOE ~ 17 GPa). In practical terms this meant buildings in Aceh were offering a resistance to the flow of roughly 1.7 times higher than forests.

score = 0.1) and empirical semivariograms (Fig. S2) showed no indication of such spatial relationships.

Results and Discussion

The developed models (Table 3) revealed that distance from the shoreline to the settlement (D) was the main factor significantly reducing the number of casualties and structural damage ($p < 0.001$). Nevertheless, vegetation in front of the settlement (LCR_F, and particularly vegetation with a high land cover roughness coefficient, Table 1) also significantly helped to reduce fatalities ($p = 0.067$). Estimates, based on our casualty model (Table 3) with local land cover conditions (Table 1), suggested that having a forest in front of a settlement would have resulted in an average 8% reduction of casualties, whereas rubber plantations and agroforestry would have reduced casualties by 5% and 3%, respectively. In contrast, thick vegetation behind settlements (LCR_{B5}) resulted in adverse effects, increasing structural damage ($p = 0.061$) as well as casualties ($p = 0.101$). Corresponding model estimates suggest that casualties increased on average by 3% given the mean LCR_{B5} observed in the study (Table 1). Having a dense forest directly behind a village would have increased casualties by 6% compared to losses in cases with nonvegetated fields behind villages. These latter effects, although statistically not very strong, could be the result of debris created by the initial wave, trapped in dense forest vegetation and returned by the backwash, as reported by many witnesses. There was no significant effect of coastal vegetation in front of the settlement regarding structural damage ($p = 0.981$).

Table 2. Variables (not transformed) used in the models and their descriptive statistics ($N = 180$)

Variable	Mean	Std Dev.	Min.	Max.
MD—maximum flood distance (m)	2,250	850	950	4,450
STD—structural damage (%)	78	39	0	100
CASU—casualties (%)	34	31	0	95
IWH—initial water height at shoreline (m)	20	5	10	25
D—distance from the shoreline to the settlement (m)	1,200	950	50	4,400
E_F—maximum elevation in front of the settlement (m a.s.l.)	14	5	6	47
E_T—maximum elevation over the whole transect (m a.s.l.)	19	8	12	74
LCR_F—weighted average land cover roughness in front of the settlement	1,165	640	71	3,538
LCR_{B5}—weighted average land cover roughness from the settlement up to 500 m behind	914	694	0	3,444
LCR_T—weighted average land cover roughness in the transect	987	311	141	1,899

The importance of distance and the interplay of land use allocation for tsunami related coastal planning could be demonstrated using the casualties model (Table 3). Given the mean tsunami intensity in 2004 (Table 2) and existing land use (Table 1), locating settlements about 3.5 km away from the shoreline apparently could have avoided most casualties. Scenarios comparing hypothetical areas with different agricultural vegetation types in front/behind settlements—e.g., grass-rice/rubber vs. rubber/grass-rice (Fig. 3)—showed that inverted LCR_F/LCR_{B5} relationships resulted in up to 10% difference in casualty estimates. Consequently, critical distances from the shoreline to the settlement (i.e., distance where no casualties occur) can vary by up to 500 m. Best/worst case scenarios comparing high and low vegetation roughness behind the settlement (LCR_{B5}) (Fig. 4) resulted in up to 30% difference in probability of occurrence of structural damage. Nevertheless, at very short and long distances from the shore such differences between vegetation types are overridden by the influence of wave energy.

Offshore conditions (IWH) were positively related to maximum flood distance ($p = 0.044$) and casualties ($p = 0.018$) (Table 3). Higher IWH significantly increased flood extension and number of casualties. However, no significant effect of IWH on structural

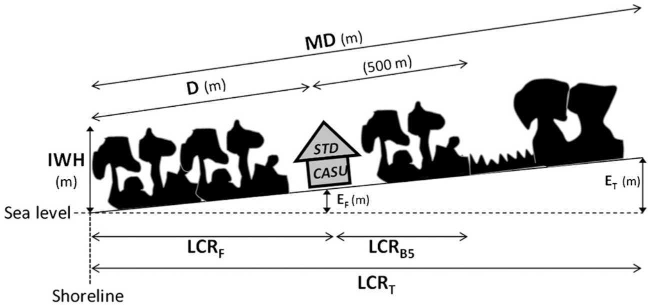

Fig. 2. Schematic transect showing the variables used in the models. MD = maximum flood distance (m), CASU = casualties (%), STD = structural damage (%), IWH = initial water height (m), D = distance from the shore line to the settlement (m) E_T = maximum elevation over the whole transect (m a.s.l.), E_F = maximum elevation at the settlement level (m a.s.l.), LCR_T = weighted average land cover roughness in the transect (up to the maximum flood distance), LCR_F = weighted average land cover roughness in front of the settlement and LCR_{B5} = weighted average land cover roughness from the settlement up to 500 m behind.

Table 3. Selected models for maximum flood distance (MD), casualties (CASU), and structural damage (STD) showing standardized regression coefficients (± standard error) and their corresponding *p* values

Model	Intercept	IWH-s	E_T-s	E_F-s	D-s	LCR_T-s	LCR_F-s	LCR_{B5}-s	AIC*	X^2/Df†
MD	0.53 ± 0.05 ($p < 0.001$)	0.62 ± 0.31 ($p = 0.044$)	−0.32 ± 0.09 ($p = 0.001$)			0.06 ± 0.06 ($p < 0.351$)			**−503**	
CASU	0.38 ± 0.04 ($p < 0.001$)	1.14 ± 0.46 ($p = 0.018$)		−0.19 ± 0.21 ($p = 0.368$)	−2.40 ± 0.36 ($p < 0.001$)		−0.38 ± 0.21 ($p = 0.067$)	0.28 ± 0.17 ($p = 0.101$)	**−117.3**	
STD	2.66 ± 0.41 ($p < 0.001$)	3.45 ± 3.73 ($p = 0.358$)		−4.95 ± 3.35 ($p = 0.143$)	−22.42 ± 4.40 ($p < 0.001$)		0.13 ± 5.14 ($p = 0.981$)	6.90 ± 3.62 ($p = 0.061$)		**1.07**

Generalized linear mixed model using a spatial variance-covariance model fitted by a random term. Estimation technique for MD and CASU: maximum likelihood (ML). Estimation technique for STD: pseudolikelihood (PL). $N = 180$.

All independent variables used in the models were standardized (suffix "-s") to variance = 1, mean = 0.

IWH-s = initial water height, **E_T-s** = maximum elevation over the whole transect, **E_F-s** = maximum elevation at the settlement level, **D-s** = distance from the shoreline to the settlement, **$\sum LCR_T$-s** = cumulative land cover roughness in the transect, **LCR_F-s** = weighted average land cover roughness in front of the settlement, and **LCR_{B5}-s** = weighted average land cover roughness up to 500 m behind the settlement.

*Akaike information criterion.

†Chi square/degrees of freedom.

damage was detected ($p = 0.358$). This was most likely due to the extreme force of the waves in west Aceh, being only 150 km away from the epicenter with wave heights up to 25 m. In contrast to other areas (2, 4), even the reported minimum IWH (10 m) was sufficient to cause total damage to structures close to the shore. While buildings were fully exposed to the force of the waves, peoples' chances to escape increased at lower wave height.

The lack of significance of topography (E_F) in the casualties ($p = 0.368$) and structural damage ($p = 0.143$) models (Table 3) might have been due to the small elevation changes on site (Table 2). A different result was shown for the maximum flood distance model where elevation changes were more relevant ($p = 0.001$) together with IWH (Table 3). LCR_T showed no significant impact on flood distance. This suggested that a tsunami wave travels as far as the elevation bounds but may go slower if there are obstacles set by vegetation.

Claims of vegetation helping people to escape have also been documented in other studies (3, 28, 29), including the concept of "soft landing" (28). A moderate positive impact of vegetation on the chances of saving human lives was confirmed in our study but only with respect to land cover in front of settlements. Nevertheless, the current study also showed that an increase in land cover roughness behind a settlement (LCR_{B5}) was positively related to an increase in casualties, indicating an adverse effect (Table 3). This relationship may also indicate that people washed into forested areas, either against trees or places with high LCR, had lower survival chances (*ca.* −3%, based on our mean model estimates for the study area) than those washed into places with low LCR or open areas. These results are in agreement with observations by other studies mentioning that vegetation in Thailand may have created fatal barriers between the shoreline and higher ground hindering people's ability to escape (30).

Thus, vegetation can induce different impacts depending on its occurrence and shape in front and behind villages. Hence, the difference in data distribution between LCR_F and LCR_{B5} (Fig. 5) explains why an overall decrease in casualties in the study area was possible given the higher weighted average roughness in front of settlements against a relatively lower one behind. In terms of future costal planning this would suggest that it is preferential to plant productive agroforests in front of communities while cropping fields would be allocated behind villages.

Observations along the coast of Kerala, India, showed that not even concrete walls protected the coast from the 2004 tsunami impact (15), yet at the same time bioshields were recommended for tsunami hazard mitigation. Our research suggests that, under extreme conditions as in west Aceh and without mangrove forests, coastal vegetation between the shoreline and a settlement reduced casualties, probably diminishing water speed and allowing people to escape, which would explain why such effect was not observed for structural damage.

Earlier assessments also included land and vegetation effects on water flows, especially floods (6, 19, 20), but their procedures to quantify such effects were more complex and data demanding. Our approach accounts for the resistance of vegetation opposing flow, expressed in volumetric units (diameter, height, density) as

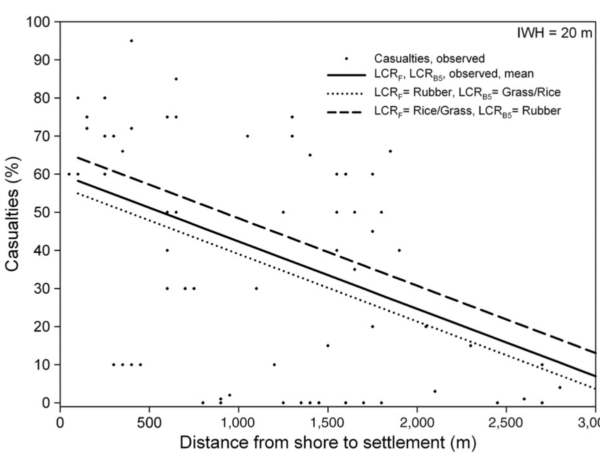

Fig. 3. Predicted (lines, CASU model, Table 3) and observed (symbols) change in percentage of casualties with distance from shoreline to settlement (D) at average initial water height (IWH) of 20 m. Three model scenarios of weighted average land cover roughness in front of the settlement (LCR_F) and weighted average land cover roughness from the settlement up to 500 m behind (LCR_{B5}) were used.

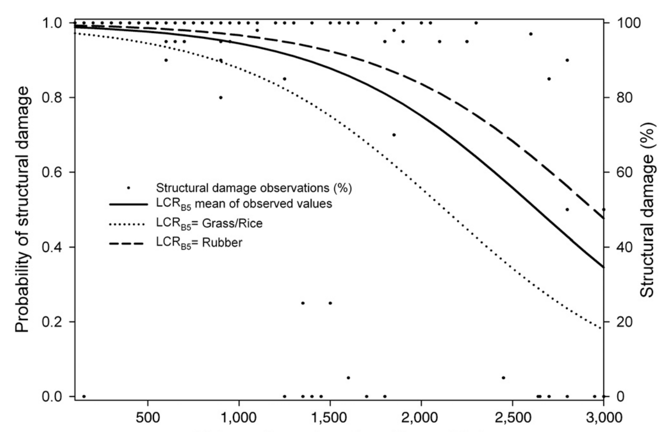

Fig. 4. Probability of structural damage with distance from shoreline to settlement (D) (lines, STD model, Table 3) over all initial water height (IWH) values. Three scenarios of weighted average land cover roughness from the settlement up to 500 m behind (LCR_{B5}) were employed. Symbols represent observed structural damage (%).

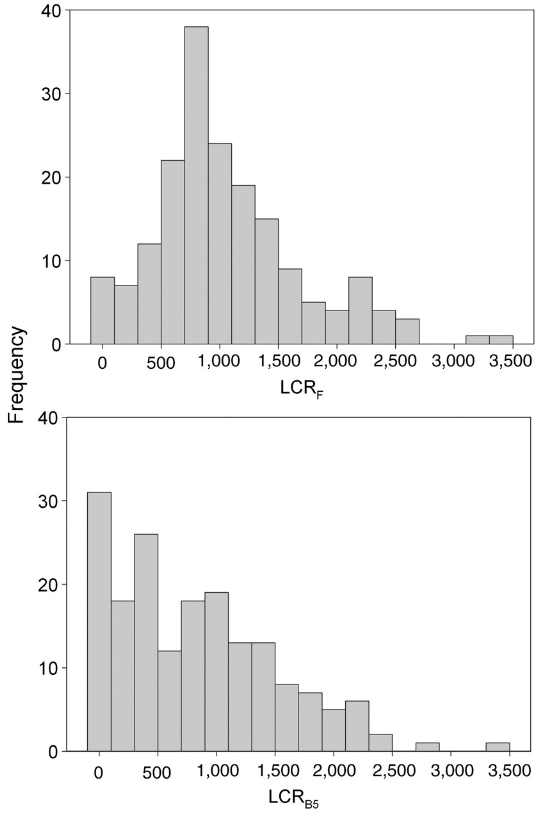

Fig. 5. Histogram comparison for (*A*) weighted average land cover roughness in front of the settlement (LCR$_F$) and (*B*) weighted average land cover roughness from the settlement up to 500 m behind (LCR$_{B5}$).

a vegetation resistance coefficient (VR). Once VR was combined with different land covers and their areas, the LCR coefficient allowed a landscape level assessment. This approach enabled grouping land covers such as “forest” and “rubber,” which have similar height and density but differ due to the typically higher average diameter of forest stems than rubber. A more comprehensive resistance factor might include elements such as Manning’s resistance coefficient and the Darcy–Weisbach friction factor as well as differences in flow speed and resistance of submerged and nonsubmerged vegetation (19, 20). Although the use of such characteristics may produce a more mechanistic model, the approach proposed here provides an assessment that facilitates coastal planning based on readily available data. Despite our measurements of height, stem diameter, and planting density being made in posttsunami conditions using similar land cover types, albeit not affected by the tsunami, we believe the values were an adequate representation of pretsunami conditions.

The present damage evaluation focused on casualties and structural damage, similar to other studies (2, 4, 5, 11), but it considered criticism that some of these had received (7–10, 18). Issues regarding spatial autocorrelation in assessment methods were addressed through the use of a spatially explicit statistical model. Factors discarded by other authors, such as topographic changes (12), were included. Offshore factors such as bathymetry, distance to epicenter, and slope of the island (proximal and distal) were represented through IWH. The multivariate models allowed us to focus specifically on inland factors and filter out vegetation effects. Despite distance being the overall factor determining damage, the effects of land cover roughness in the models was statistically confirmed at $\alpha = 0.1$.

Tsunamis of a magnitude like the 2004 event are relatively rare (31). Nevertheless, recent events such as the one in Japan on March 2011 and the February 2010 earthquake in Chile show that these threats are real and require preparedness and adequate policy responses. Unsubstantiated statements regarding protection provided by coastal vegetation can be obstructive and even dangerous. More critical investigation, including spatial multivariable approaches, must be encouraged in order to determine criteria for successful mitigation measures, including debris effects.

Our main conclusion that distance to the shoreline (D) most effectively reduced casualties and structural damage (Table 3) implies that settlements should be preferentially located away from the shoreline and at an elevated position (although in the case of the study area there was limited scope to chose higher elevated areas close to the shoreline). However, in practical terms, a coastal planning strategy that aims only to locate settlements away from coastlines is likely to fail. For local villagers, closeness to the sea not only represents danger but also potential income generation opportunities and food security. Thus coastal planning must consider additional attenuating and mitigation effects of coastal vegetation such as the demonstrated reduction of casualties provided by agroforests in front of settlements having a large vegetation roughness coefficient (LCR$_F$). Because of the only moderate effectiveness and associated uncertainties of coastal vegetation against tsunami effects, its composition must be based upon its wider livelihood context not only its mitigation role (e.g., bioshields). Allocation of more dense agroforests in between sea and communities (i.e., cacao, rubber and multilayered home gardens) yielding tangible benefits for farmers should be an important spatial planning measure. Additionally, cropping fields that do not trap people while they try to escape (i.e., rice, agriculture) should be located behind settlements. These interventions should consider local ecological niches and customs.

In order to reduce vulnerability and to have lasting benefits, strategic planning thus must consider strengthening livelihoods via satisfaction of local needs and preferences (32) as well as provision of environmental goods and services. Economically valuable tree crops such as rubber and agroforests can potentially satisfy these requirements. Risk management planning thus must consider adequate distribution of settlements but also of productive areas, and it must take into account the potential negative impact of dense vegetation behind communities. Because of the limited effectiveness of vegetation toward large tsunamis, additionally appropriate risk mitigation actions such as early warning systems need to be implemented (30). Only a combination of these measures will provide hazard reduction and mitigation as well as food security and sustainable development opportunities.

Methods

Maximum flood distance (m), casualties (%), and structural damage (%) were used as proxies for tsunami energy and tsunami damage indicators. Impact data were collected in the districts of Aceh Barat, Nagan Raya, and Aceh Jaya, along more than 110 km of shoreline south of the city of Calang. Settlements where damage was registered were geo-referenced. Semistructured interviews in 49 coastal communities were carried out to gather primary information on damage indicators and land cover changes. Structural damage was calculated from the number of buildings left standing after the tsunami. Maximum water height was determined by measuring references mentioned during the interviews (e.g., houses, palm trees, or overland electricity lines) with a clinometer.

To assign pretsunami plant parameters of different land uses, vegetation density, stem diameter (at breast height for tree-type vegetation or ground level for smaller types), and height were measured using a clinometer and measuring tape and then averaged for each land use type. The assessment was done in 2008–09 on corresponding plots adjacent to the tsunami affected zone. Two high-resolution pretsunami images (Quick Bird®, 2.5 m) were compared to posttsunami imagery in order to identify similar land uses inside and adjacent to tsunami affected areas. According to interviews and satellite imagery, the plantation techniques and designs for major tree crops as well as food crops followed a standard pattern in the investigated region. Additionally, for the tree crops such as coconut and rubber, plant parameters were measured on 0.5 ha plots for each land cover type with comparable age classes as before the tsunami. A transect across each plot was used and all trees in at least two subplots of 10×10 m were measured and averaged. Pretsunami land cover classification of the area was based on a 2002 Landsat® imagery and identified 13 types of land use. The area was covered by a mosaic of tree-crop plantations, agroforests, and rice fields. Approximately half of the study area included trees like coconut (20%), rubber (17%), agroforests and forests (7%), and oil palm plantations (6%) (Table 1).

The initial impact data were collected in 2007 (24 communities, approximately 60 km of shoreline) and expanded following the same methodology during a second campaign (25 communities, over 50 km of shoreline) in 2008. Posttsunami satellite imagery (Quickbird® 5 m resolution, 2004) and data from different agencies were used to cross-check field information. Navigation charts were used to visually verify homogeneity of coastal geomorphology and factors such as absence of reefs. Similar near-shore bathymetrical variability along the studied coast were also observed. For each observation point where damage indicators were determined in a village, transects 550 m wide extending from the shoreline through the settlement location to the maximum flooded area were superimposed (Fig. 1). Measurements of distance to the shoreline, elevation (Digital Elevation Model—Shuttle Radar Topographic Mission http://www2.jpl.nasa.gov/srtm/) and land cover friction coefficients in front of and behind settlements were allocated to these transects ($N = 180$).

Generalized linear mixed models allowed fitting the spatial autocorrelation of observations distributed along the coastline. The coordinates of each observation were used to fit a spatial variance-covariance model across all observations using a spherical covariance structure for all the models. The procedure was also run as a logit link/binomial and an identity link/normal model for binary and quantitative responses, respectively. Spatial covariance was entered via a random effect in the linear predictor (27). The normal model was fitted using maximum likelihood (ML) in order to compare models of the same dependent variable with different fixed effects by AIC (33). Models explaining the respective damage indicators were defined by Eqs. **4**, **5**, and **6**. Explanatory variables considered were initial water height (IWH) representing initial tsunami magnitude and energy at shoreline given by offshore characteristics; elevation above sea level (E) representing gravity and weighted average LCR coefficient representing wave resistance by vegetation. Distance from the settlement to the shoreline (D) was entered as an additional predictor to test for the effects correlated to other predictors where LCR_F and LCR_{B5} were used. Response variables representing the damage caused by the waves were casualties (CASU), structural damage (STD), and maximum flood distance (MD). A stepwise procedure was used to test the improvement of the model by sequentially introducing the terms LCR_F and LCR_{B5} in the corresponding models (Tables S1 and S2). Final equations are shown in Table 3. Comparison of different model approaches showed that the fit of individual (single) predictor models (Tables S3 and S4) was poorer than that for models including all variables (Table 3). Pearson pairwise correlation tests run among all predictors yielded only weak correlations. Normality of the residuals for the casualties and maximum flood distance models was checked using *q-q* plots. GIS and statistical analyses were carried out using a combination of the packages Open Jump 1.2, ArcGIS 9.2, ArcView 3.2, SAS 9.2 (PROC GLIMMIX), and Sigmaplot 10.0. Data was collected and geo-referenced in the field with a GPS Garmin® GPSMAP 76CSx.

ACKNOWLEDGMENTS. We thank the German Aerospace Center for support on imagery management; the Pacific Disaster Center for providing satellite imagery; Andree Ekadinata from the World Agroforestry Centre Southeast Asia Program for Landsat® land cover classification and general GIS support; the Rehabilitation and Reconstruction Agency (BRR-Indonesia), Red Cross International and BPS-Statistics Indonesia for secondary damage information; the Federal Institute for Geosciences and Natural Resources, Hannover, Germany for GIS support; the chiefs and inhabitants of the villages in the study for their participation; Dr. Juan Guillermo Cobo and Betha Lusiana for their contributions to the statistical analysis; Dr. Lucy Rist for commenting on earlier drafts of the manuscript; Rob Finlayson and Scott Demyan for improving English redaction; A. Firdaus, D. Herlita, Y. Astuti, and W. Angkasa for data collection support. We thank the reviewers for their thoughtful insights on previous versions of this manuscript. Research funded by Eiselen Foundation; ReGrIn project, EU Asia Pro Eco IIB program; and GTZ on behalf of the government of the Federal Republic of Germany.

1. Stein S, Okal EA (2005) Speed and size of the Sumatra earthquake. *Nature* 434:581–582.
2. Danielsen F, et al. (2005) The Asian tsunami: A protective role for coastal vegetation. *Science* 310:643.
3. Tanaka N, Sasaki Y, Mowjood MIM, Jinadasa KBSN, Homchuen S (2007) Coastal vegetation structures and their functions in tsunami protection: Experience of the recent Indian Ocean tsunami. *Landsc Ecol Eng* 3:33–45.
4. Olwig MF, et al. (2007) Using remote sensing to assess the protective role of coastal woody vegetation against tsunami waves. *Int J Remote Sens* 28:3153–3169.
5. Kathiresan K, Rajendran N (2005) Coastal mangrove forests mitigated tsunami. *Estuar Coast Shelf Sci* 65:601–606.
6. Latief H, et al. (2007) The role of forests and trees in protecting coastal areas against tsunamis. *Regional Technical Workshop on Coastal Protection in the Aftermath of the Indian Ocean Tsunami What Role for Forests Trees?*, eds S Braatz, S Fortuna, and J Broadhead (FAO, Rome), pp 5–32.
7. Kerr AM, Baird AH (2007) Natural barriers to natural disasters. *Bioscience* 57:102–103.
8. Baird AH, Bhalla RS, Kerr AM, Pelkey NW, Srinivas V (2009) Do mangroves provide an effective barrier to storm surges? *Proc Natl Acad Sci USA* 106:E111.
9. Baird A, Kerr A (2008) Landscape analysis and tsunami damage in Aceh: Comment on Iverson and Prasad (2007). *Landsc Ecol* 23:3–5.
10. Young E (2006) Is replanting coasts the way to protect against tsunamis? *New Sci* 189:14–14.
11. Iverson LR, Prasad AM (2007) Modeling tsunami damage in Aceh: A reply. *Landscape Ecol* 23:7–10.
12. Kaplan M, Renaud FG, Lüchters G (2009) Vulnerability assessment and protective effects of coastal vegetation during the 2004 tsunami in Sri Lanka. *Nat Hazard Earth Syst* 9:1479–1494.
13. Geist EL, Titov VV, Synolakis CE (2006) Tsunami: Wave of change. *Sci Am* 294:56–63.
14. Iverson LR, Prasad AM (2007) Using landscape analysis to assess and model tsunami damage in Aceh province, Sumatra. *Landsc Ecol* 22:323–331.
15. Kurian NP, Pillai AP, Rajith K, Murali Krishnan BT, Kalaiarasan P (2006) Inundation characteristics and geomorphological impacts of December 2004 tsunami on Kerala coast. *Curr Sci* 90:240–249.
16. Chadha RK, Latha G, Yeh H, Peterson C, Katada T (2005) The tsunami of the great Sumatra earthquake of M 9.0 on 26 December 2004—impact on the east coast of India. *Curr Sci* 88:1297–1301.
17. Shuto N (1987) The effectiveness and limits of tsunami control forests. *Coast Eng Jpn* 30:143–153.
18. Dahdouh-Guebas F, et al. (2005) How effective were mangroves as a defense against the recent tsunami? *Curr Biol* 15:R443–R447.
19. Freeman GE, Rahmeyer WH, Copeland RR (2000) *Determination of Resistance Due to Shrubs and Woody Vegetation* (U.S. Army Corps of Engineers, Engineer Research Development Center, Vicksburg, MS), ERDC/CHLTR-00-25.
20. Järvelä J (2004) Determination of flow resistance caused by non-submerged woody vegetation. *Int J River Basin Management* 2:61–70.
21. Peltola H, Kellomäki S, Hassinen A, Granander M (2000) Mechanical stability of Scots pine, Norway spruce and birch: an analysis of tree-pulling experiments in Finland. *For Ecol Manage* 135:143–153.
22. Chan TK, Lim SH, Tan HTW, Lim CP (1999) Variation of bending capacity along the lamina length of a grass, Imperata cylindrica var. major (Gramineae). *Ann Bot* 84:703–703.
23. Oladokun M (2006) Structural development and stability of rice Oryza sativa L. var. Nerica 1. *J Exp Bot* 57:3123–3130.
24. Toledo E, Rincón C (1997) Use of new forestal species in Peru (Utilización industrial de nuevas especies forestales en Perú). *Revista Forestal Centroamericana* 21:31–36.
25. Tomosawa F, Noguchi T (1993) Relationship between compressive strength and modulus of elasticity of high-strength concrete. *Proceedings of the Third International Symposium on Utilization of High-Strength Concrete* (Norwegian Concrete Assn, Lillehammer, Norway), pp 1247–1254.
26. Boen T (2006) Observed reconstruction of houses in Aceh seven months after the great Sumatra earthquake and Indian Ocean tsunami of December 2004. *Earthq Spectra* 22:S803–S818.
27. Schabenberger O (2005) Introducing the GLIMMIX procedure for generalized linear mixed models. *Proceedings ofthe Thirtieth Annual SAS Users Group International Conference* (SAS Inst Inc, Cary, NC).
28. Tanaka N (2009) Vegetation bioshields for tsunami mitigation: Review of effectiveness, limitations, construction, and sustainable management. *Landsc Ecol Eng* 5:71–79.
29. Dengler L, Preuss J (2003) Mitigation lessons from the July 17, 1998 Papua New Guinea tsunami. *Pure Appl Geophys* 160:2001–2031.
30. Cochard R, et al. (2008) The 2004 tsunami in Aceh and Southern Thailand: A review on coastal ecosystems, wave hazards and vulnerability. *Perspect Plant Ecol Evol Syst* 10:3–40.
31. Monecke K, et al. (2008) A 1,000-year sediment record of tsunami recurrence in northern Sumatra. *Nature* 455:1232–1234.
32. Ziegler AD, Wong PP, Grundy-Warr C (2009) Still vulnerable to killer tsunamis. *Science* 326:1188–1189.
33. Burnham KP, Anderson DR (2002) *Model Selection and Multimodel Inference. A Practical Information Theoretic Approach* (Springer, New York).

ENVIRONMENTAL SCIENCES

SUSTAINABILITY SCIENCE